

Novel Nonflammable Electrolytes for Secondary Magnesium Batteries and High Voltage Electrolytes for Electrochemical Supercapacitors

SBIR Phase II Final Technical Report
Award No. DE-FG02-04ER84040

In Response to DoE SBIR FY 2004 Topic 31b

Submitted to:

U.S. Department of Energy
Office of Sciences
Chicago Office
9800 South Cass Avenue
Argonne, Illinois 60439

Submitted by:

Dr. Brian Dixon
Phoenix Innovation, Inc.
PO Box 550
Wareham, Massachusetts 02576

December 30, 2007

Table of Contents

	<u>Page</u>
1.0 INTRODUCTION	1
2.0 PHASE II WORK CARRIED OUT	2
2.1 Magnesium Battery Experimental	2
2.1.1 Electrolyte Synthesis	2
2.1.2 Synthesis of Vanadium Phosphate Cathode Material	3
2.1.3 Magnesium/Lithium Alloy Formation	4
2.2 Results	4
3.0 MAGNESIUM BATTERY EFFORT CONCLUSIONS AND RECOMMENDATIONS	17
4.0 SUPERCAPACITOR RESEARCH EFFORT	18
4.1 Results & Discussion	19
5.0 CONCLUSION	26

List of Tables and Figures

	<u>Page</u>
Tables	
Table 1: Composition of Test Electrolytes	5
Table 2: Representative Electrolyte Conductivities (22°C)	20
Figures	
Figure 1: CV of Mg and Mg Alloy vs Mg/Mg ⁺ 50 mV/sec SR Pt WE electrolyte: 0.2M MgIm in 2-80-2 SM519-1 electrolyte (MgIm)	7
Figure 2: Mg vs MgLi (19%), Pt WE, SR = 50 mV/sec (voltages vs Mg/Mg ⁺²)	8
Figure 3: CV of Mg with Arc cathode and Mg with Ag cathode vs Mg/Mg ⁺ 50 mV/sec SR Pt WE 02 M MgIm in 2-80-2	9
Figure 4: CV of optimized electrolytes to determine relative Mg salt activity	10
Figure 5: Cycling of Mg, BCNT cell using Electrolyte 494-2 C/D @ 100 microamps	11
Figure 6: Comparison of the performance of two MgIm salts	12
Figure 7: MgTf salt with AgO cathode D @ 100 microamps C @ 25 microamps	12
Figure 8: Cycling of a commercial solvent/ MgIm electrolyte	13
Figure 9: Electrolyte 494-3' Anode versus a Fresh Mg Anode.	14
Figure 10: MgLi Alloy anode Initial Cycle	15
Figure 12: AZ91 Anode Initial Cycle	16
Figure 13: AZ91 Anode Subsequent Cycling	16
Figure 14: Ionic Liquid Electrolyte/Magnesium Cell	17
Figure 15: CV of Experimental Electrolyte	21
Figure 16: Comparison of CVs for Test and Control Electrolytes	21
Figure 17: 1M Lithium Salt in Acetonitrile, Control	22
Figure 18: Chronopotentiometric Tests of Various Electrolytes	23

Figure 19: Experimental Electrolyte charged to 9.8 V

24

Figure 20: Modified Experimental Electrolyte

25

1.0 INTRODUCTION

Magnesium electrochemical systems have not received the attention their promise justifies ^{1, 2,3,4} Aurbach, among others, has demonstrated and championed the promise of magnesium secondary battery technologies.^{5 6} However, to date the majority of the promising work involving magnesium revolved around the use of materials, such as Grignard reagents, that present the same set of safety and instability problems encountered with lithium. In this case there would be no advantage to using magnesium. Magnesium and lithium are complementary systems. Although magnesium runs at a substantially lower voltage than lithium, the metal is inherently much safer. Lithium batteries are clearly the focus of a great deal of research and commercial development because of the attractive high energy and power density of lithium systems. However, along with these enviable characteristics come substantial drawbacks. In particular, safety is much more of a concern, as well as shelf stability. These concerns recently led the USDOT to ban shipping of lithium cells by passenger aircraft.⁷ The high reactivity of lithium requires non-aqueous, aprotic electrolytes in order to preclude undesirable side reactions of lithium, and to control its explosive nature. In instances of abuse, reactive liquid electrolyte products have been implicated as a source of explosions in secondary lithium batteries. In primary batteries, such as Li/SOCl₂, even in cases of no abuse, reactive intermediates have been known to cause partially discharged batteries to explode. Also, the high energy of lithium batteries makes self-discharge an issue. For instance, the 18650 Li-ion battery will lose up to 20% of its capacity per year stored at 20° C. Successful development of alternative, complimentary, systems would afford greater flexibility to equipment developers and consumers in choosing a battery. In this regard, magnesium is an attractive anode material because of its high charge density (low electrochemical equivalence) and considerably negative electrode potential (-2.37V vs. NHE). In comparison to lithium it is more attractive because it is less expensive and much safer. Although safer than lithium, Mg is still reactive with water so that non-aqueous electrolytes are required for secondary batteries. Magnesium has been used successfully in primary batteries, but its use in rechargeable cells has been stymied by the lack of suitable non-aqueous electrolyte that can conduct Mg⁺² species, combined with poor stripping

and plating properties. The development of a suitable cathode material for rechargeable magnesium batteries has also been a roadblock, but a nonflammable electrolyte is key. In the Phase I work we have established the promise of our proposed nonflammable polyphosphonate electrolytes for secondary magnesium systems. In Phase II we intended to expand upon this promise by optimizing this family of electrolytes, as well as the accompanying anodes and cathodes.

In addition to exploring the utility of these novel electrolytes for use in secondary magnesium batteries, in a cooperative effort with the Missile Defense Agency, we explored the use of these electrolytes in electrochemical supercapacitors. The goal of this portion of the research and development effort was to determine if novel supercapacitor electrolytes could be formulated that possessed voltage stabilities of 8-10V. More specifically, Phoenix Innovation was to prepare a series of phosphonate electrolytes that were then to be screened for stability as a function of voltage.

2.0 PHASE II WORK CARRIED OUT

2.1 Magnesium Battery Experimental

2.1.1 Electrolyte Synthesis

The key component of the experimental electrolytes was the solvent system used in conjunction with the supporting electrolyte; i.e. magnesium salts. We chose to examine two different magnesium salts for this Phase II work. The first is a readily available commercial product, magnesium trifluoromethane sulfonate or MgTf, while the second is a specialty product, magnesium trifluoromethane sulfonimide or MgIm. The MgTf was purchased from Aldrich Chemical Co. and used as received without further purification. A 2 g quantity of MgIm was initially purchased from Covalent Associates (Woburn, MA.) and following its expenditure, additional MgIm was synthesized using the following procedure:

The synthesis was carried out in a dry box because of the moisture sensitivity of the reactants. Bis-trifluormethane sulfonamide (5.4g, 271g/mole) was dissolved into 50 mL of exquisitely dry methylene chloride. Dibutyl magnesium (1.37g; 138.5g/mole; 1M solution in hexane) was

added dropwise via syringe to this mixture. The white precipitate was isolated by vacuum filtration, washed with dry CH_2Cl_2 and dried under high vacuum.

Solvents for preparing the experimental electrolytes were primarily polyphosphate-based materials. A variety of commercial and synthetic solvents were employed to prepare experimental electrolytes. Among the choices, the commercially available solvents included: diethyl-1-propane phosphonate, diethyl bromoethyl phosphate dimethyl methyl phosphonate and trimethyl phosphate. Synthetic solvents included polyphosphate materials synthesized in-house.

In addition to magnesium salts as solutes in the electrolyte, several electrolytes were prepared which included the addition of ionic liquids such as butylmethylimidazolium trifluoroborate (BMITFB) or ethyltriphenyl phosphonium bromide (ETPPB) which were added in small quantities to several electrolytes in an attempt to improve the Mg^{+2} transport through the electrolyte. These ionic liquids were purchased from either Aldrich Chemical Co. or Strem Chemical Co. and used as received.

2.1.2 Synthesis of Vanadium Phosphate Cathode Material

In a typical preparation the lithium vanadium phosphate was prepared by mixing stoichiometric amounts of $\text{NH}_4\text{H}_2\text{PO}_4$, V_2O_5 , and Li_2CO_3 . The mixture was initially heated to 300 °C in air for 4 h to allow H_2O and NH_3 to evolve. The resulting product was then ground and heated in 1 hour, 200°C step, to 850 °C under a stream of pure hydrogen for 8 h. An alternative preparation method involved carbo-thermal reduction (CTR) using carbon as the reducing agent, but substituting Mg for Li. (Electrochem. Solid-State Lett., Volume 6, Issue 3, pp. A53-A55, March 2003).

2.1.3 Magnesium/Lithium Alloy Formation

An attempt was made to prepare Mg/Li alloys reasoning that the lithium in the alloy might help overcome the passivation of the Mg by electrolyte during charging. In an attempt to prepare alloys of Mg and Li, we first weighed out a specific quantity of pure magnesium chunks and added to this a specific quantity of pure lithium pellets. All of this work was conducted in a dry, Ar-filled glovebox. The weight of lithium in the mixtures ranged from 10 w/o to 30 w/o. After

mixing the two metals, we placed them in a screw-type mold and tightened both rams to squash the mixture. The mold was then removed from the glovebox and heated to 800° C for 20 minutes in a tube furnace under Ar. The mold was removed from the tube furnace, cooled and the product was then removed from the mold. In most cases, the product represented about 30% of the original mass of the mixture. It appeared that the lithium had vaporized and condensed downstream from the mold attacking the quartz tube in the process. We collected what product we could from these trials and stored them under Ar until needed.

2.2 Results

Summary:

The goal of this effort was to identify nonflammable electrolyte alternatives for magnesium secondary batteries. In attempting to achieve this goal, we covered much ground and strayed from our usual discipline of changing one system variable at a time. What resulted is a glimpse of what may eventually prove to be a better secondary magnesium battery system.

The better electrolytes exhibited ionic conductivities in the range of 5×10^{-4} to 1×10^{-3} S/cm. These conductivities were sufficient to support cycling of various combinations of metal anodes and cathodes. Initially we investigated the use of pure magnesium anodes versus metallic silver and silver oxide cathodes. These experiments demonstrated that the system functioned well enough to support cell voltage (at 50 microamp discharge) of around 0.5V for at least ten cycles. Subsequent experiments using carbon nanotube (CNT) cathodes and CNT/vanadium phosphate cathodes resulted in higher cell voltages (~1.4V) and higher rates (100 microamps) for longer discharge times (3 hours). Experiments employing anodes other than pure magnesium resulted in better performance, in some instances. Anodes composed of mixtures (possibly alloys) of Mg and Li yielded higher cell voltages, but poor cycle performance. A commercial alloy (AZ91) appeared to yield the best results from the standpoints of both cell cycling and cell voltage. Since we were simultaneously varying the electrode pairs and attempting to identify a workable system, the results appear somewhat haphazard. However, what is clear from this work is that phosphate ester solvents, together with MgIm salts form a workable, nonflammable electrolyte that is capable of supporting cell capacities in excess of 100mAh/g at cell voltages in the range

of 1 to 1.5 volts. These results are superior to those reported to date in the literature⁴ for flammable THF-based electrolytes.

2.2.1 Conductivity Measurements

Conductivity measurements of the test electrolytes were conducted using our standard two electrode test cell where stainless steel blocking electrodes served as the electrical contacts and a single piece of nonwoven glass separator contained the test electrolyte. A Phillips model 6330 RCL meter was used to measure the AC resistance of the electrolyte. This measurement was then converted to conductivity based on the dimensions of the electrodes, the separation distance etc. The conductivity was then expressed in S/cm based on the calculation:

$$\sigma = L/R A$$

where:

L = distance between the electrodes

R = measured resistance in ohms

A = area of the electrodes

The following table summarizes the composition and resulting conductivity of several of the better experimental electrolytes.

Table 1: Composition of Test Electrolytes

Electrolyte	Salt	Concentration	Solvent	IL	Conductivity (S/cm)
SM481-1	MgIm	0.13M	SM481-1E	-	1x10 ⁻³
SM481-3	MgTf	0.25M	SM481-1E	ETPPBr	1x10 ⁻⁴
SM487-2E	MgTf	0.25M	SM481-1E		1x10 ⁻³
SM487-3E	MgTf	0.25M	SM481-1E	ETPPBr	1.3x10 ⁻³
SM488-1	MgTf	0.37M	SM481-1E	0.6g BMITFB	5x10 ⁻⁴
SM490-1	MgIm, CA	0.13M	BMG2-80-2		1x10 ⁻³
SM492-1	MgTf	0.59M	BD7-24		Not soluble
SM492-2	MgIm CA	0.21M	BD7-24		8x10 ⁻⁴
SM492-4	MgIm CA	0.21M	bd7-20ix		
SM493-4	MgIm, CA	0.21M	bd8-52		5x10 ⁻⁴
SM494-1	MgIm, CA	0.21M	DE-1-PP		5x10 ⁻⁴
*SM494-2	MgIm, CA	0.21M	DEBrEP		2x10 ⁻³
*SM494-3'	MgIm	0.32M	DEBrEP		1x10 ⁻³
SM521-2	MgIm bd8-73	0.21M	DE-2-Br-P		3x10 ⁻⁴
SM522-1	MgTf	0.22M	SM481-1E		9x10 ⁻⁴ fully dissolved
SM522-2	MgTf	0.31M	Bd8-6		1x10 ⁻⁴ Partially dissolved
SM522-2-1	MgTf	0.24M	BD8-6 + 30% 2-80-2		3x10 ⁻⁴

SM526-3	MgIm	0.24M	SM481-1E		1.62x10 ⁻⁴
SM526-4	MgIm CA	0.24M	Sm481-1E		3x10 ⁻⁴

*Brominated solvent appears to be needed to effect good cycling of Mg, but a combination of this and the PEG P is needed as evidenced by the fact that the pure Diethyl bromopropane Phosphonate with MgIm doesn't work as well. As can be seen from this table, many of the candidate solvents failed to dissolve the select magnesium salts. As an example, electrolyte SM 522-2 which consisted of MgTf and solvent bd8-6 resulted in only partial dissolution of the magnesium salt. In this instance, the solvent was a PEG 450 phosphate which appeared to be less than adequate in dissolving the MgTf. This is contrasted with electrolyte SM 487-2E which contained solvent SM481-1E which was a 90:10 (wt:wt) mixture of bd8-6 and BMG 280-2. The latter solvent was a synthesized material that contained a halogenated phosphate ester. This particular solvent proved to be one of the better materials for dissolving MgTf. As can be seen from this table, the conductivity of the resulting electrolyte was quite respectable (1x10⁻³ S/cm). Interestingly, the halogenated phosphate ester solvent alone proved to be a poor solvent for the MgTf as evidenced by electrolyte SM 492-1. Equally important was the observation that the PEG phosphate ester solvent alone (BD8-6) was also not a particularly good solvent for the MgTf as evidenced by electrolyte SM522-2 in which the MgTf was only partially soluble. Further on this table, it was found that halogenated phosphate esters readily dissolve MgIm and that the MgIm purchased from Covalent Associates performed better than that synthesized in-house.

2.2.2 Cyclic Voltammetry of Electrolytes, Alloys and Cathode Materials

A number of cathode and anode material combinations were chosen as potential candidates for the experimental battery couples. Many combinations were explored, but the following appeared to offer better performance from the sampled group.

- Magnesium metal/Silver foil
- Magnesium metal/B-doped CNT
- Magnesium metal/Ag-doped CNT
- Magnesium alloy (AZ91)/Silver foil
- Magnesium alloy (AZ91)/B-doped CNT
- Magnesium/Li alloy/BNT-doped cathode

Anode Activity

Initial experimental exploration entailed cyclic voltammetric cycling of the various combinations to ascertain the relative activity of the various couples.

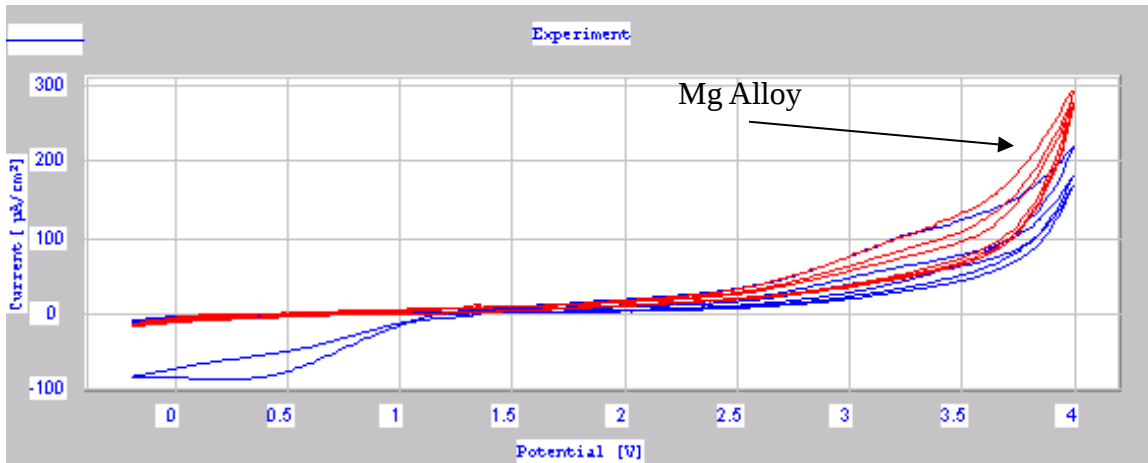


Figure 1: CV of Mg and Mg Alloy vs Mg/Mg^{+} 50 mV/sec SR Pt WE electrolyte: 0.2M MgIm in 2-80-2 SM519-1 electrolyte (MgIm)

Figure 1 depicts comparative CVs of two test cells, one containing a pure Mg electrode, the other a commercial Mg/Zn (AZ91) electrode with a Pt foil serving as a working electrode. The electrolyte in both cases was a synthesized halogenated phosphate ester (BMG2-80-2) with MgIm as the supporting salt. As detailed in the previous narrative, this electrolyte was not the optimum choice for this comparative experiment, but the results are, nevertheless, illuminating. In these experiments, the Mg and Mg alloy electrodes served as counter and reference electrodes. As can be seen, upon sweeping to positive voltages, the Mg alloy develops higher anodic currents than the pure Mg electrode indicating greater corrosion of the alloy versus the pure Mg electrode. Upon sweeping to negative potentials at which the Mg would subsequently be plated on the Pt working electrode, it would appear that the pure Mg electrode develops more current indicating preferential plating of any dissolved Mg on the Pt WE. Subsequent sweeps of the pure Mg system shows decay of the attained anodic current indicating passivation of the Mg electrode. This is also indicated in the system employing the AZ91 counter electrode, but the decrease in anodic current with subsequent sweeps is less pronounced and overall the amplitude of the current is greater than that of the pure Mg system. Subsequent cycling experiments using the AZ91 anode and the pure Mg anode and employing a suitable cathode reflected the trend observed in this comparative CV experiment. These results are summarized in Section 2.2.3.

A second experiment was conducted comparing pure Mg to a MgLi mixture (alloy?) that contained 19% Li to determine if the alloy was more or less active than the pure Mg electrode.

Identical test conditions were employed. The electrolyte contained MgIm. These results are shown below.

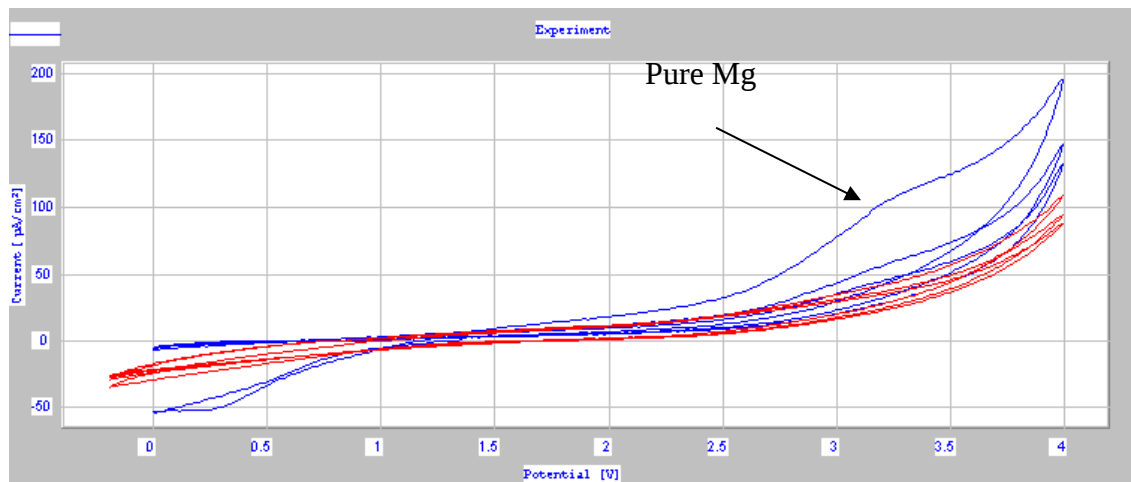


Figure 2: Mg vs MgLi (19%), Pt WE, SR = 50 mV/sec (voltages vs Mg/Mg⁺²)

The blue plot in this figure represents the CV results for the Mg electrode. As can be seen, the Mg electrode appears more active in anodically generating far greater current at positive potentials. After several sweeps, the Mg electrode appears to passivate especially in the cathodic region of the curve. There appears to be less passivation of the MgLi alloy, although its general performance seems to be less active than that of the Mg. It would appear from these results that the MgLi alloy may offer marginal improvement in anode performance over pure Mg.

Cathode Activity

In a second experiment, we compared the relative performance of a metallic silver electrode with that of a B-doped CNT electrode. Here, pure Mg served as the counter/reference electrode and the electrolyte was 0.2M MgIm in a synthesized phosphate ester solvents (BMG 2-80-2).

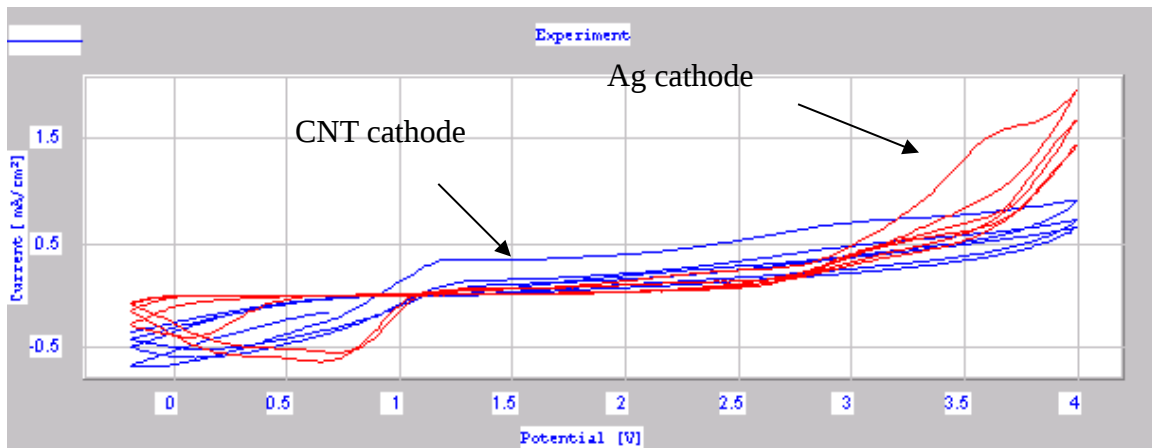


Figure 3: CV of Mg with Arc cathode and Mg with Ag cathode vs Mg/Mg⁺ 50 mV/sec SR Pt WE 02 M MgIm in 2-80-2

In this figure, the red curve is for the Ag electrode, while the blue curve represents the results using the CNT electrode. As shown, both electrodes appear to perform similarly. The exception occurs at the high anodic potentials in the case of the Ag electrode, where the current increases considerably over that of the CNT electrode. We attribute this to corrosion of the Ag electrode as it begins to occur at around 3.3V vs Mg/Mg⁺². Silver's reversible potential is 0.8V vs NHE so this would be at about the right potential versus Mg/Mg⁺². The CNT electrode appeared to generate somewhat higher currents than the silver electrode over most of the anodic potential range indicating the possibility of more activity with respect to Mg⁺² cations.

Mg Salt Activity

We conducted an experiment to compare the relative activity of the two primary salts used in these electrolytes; i.e. MgTf and MgIm. In this experiment we used a pure Mg counter/reference electrode, a metallic Ag working electrode. The electrolytes were optimized for their respective salts to ensure complete solubility. Each cell was cycled between -1.5 to 3.5V vs Mg/Mg⁺². The results of these tests are shown below.

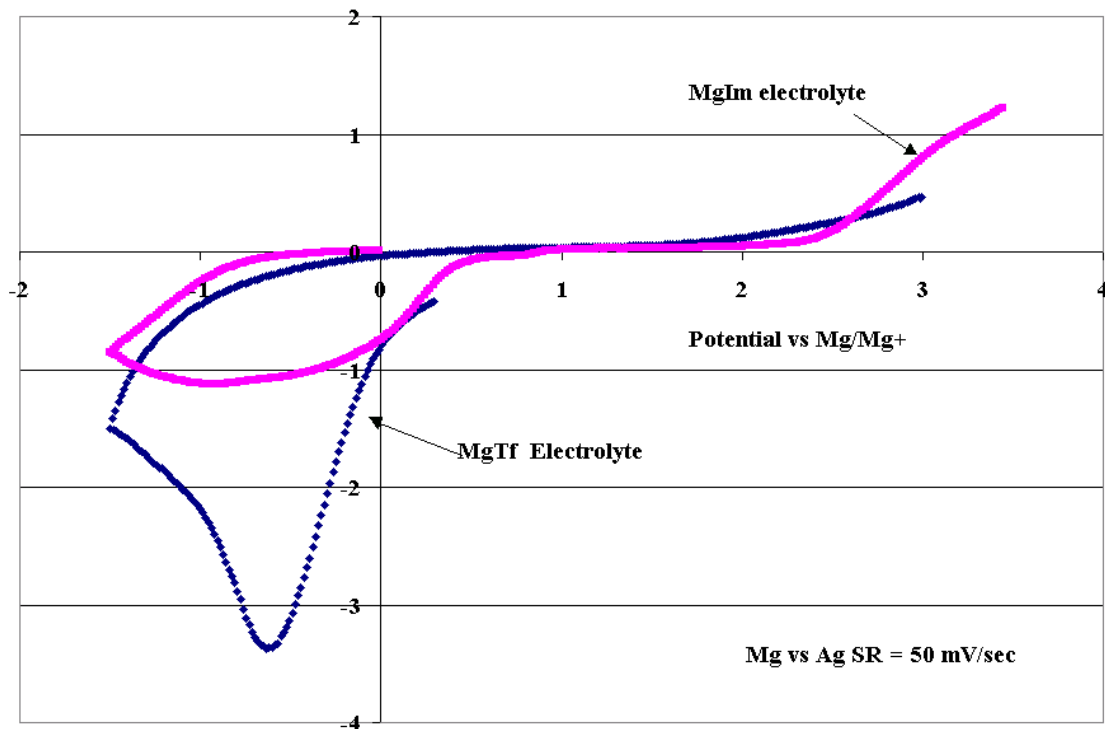


Figure 4: CV of optimized electrolytes to determine relative Mg salt activity

As can be seen in this figure, the curve representing the CV for MgIm is considerably more active in the anodic region than that for the MgTf. This would indicate greater anode corrosion in the MgIm electrolyte than in the Mg Tf electrolyte. By contrast, in the cathodic region of each sweep, the MgTf electrolyte appears to generate greater current than the MgIm electrolyte. This may indicate a passivation reaction between the MgTf and the Mg electrode at cathodic potentials. Interestingly, the cathodic current for the MgIm electrolyte is of the magnitude as the current in the anodic region of the sweep, possibly indicating plating of the corroded Mg back onto the Mg electrode. These results suggest that MgIm may be a better Mg salt than MgTf. In these phosphate ester-based electrolytes.

2.2.3 Chronopotentiometry of Various Electrode Electrolyte Combinations

Cycling of 1cm^2 Mg batteries was accomplished using a two electrode test cell employing stainless steel electrodes for contact and a steel frame to clamp the cell and provide stack pressure. All experiments were conducted on the benchtop at ambient temperature. A Radiometer Voltalab PZ301 was used to control the cell and gather data.

The first figure is representative of the results obtained using a B-doped CNT cathode and a magnesium anode. In this experiment, MgIm was dissolved in BD7-24 a brominated phosphate ester solvent.

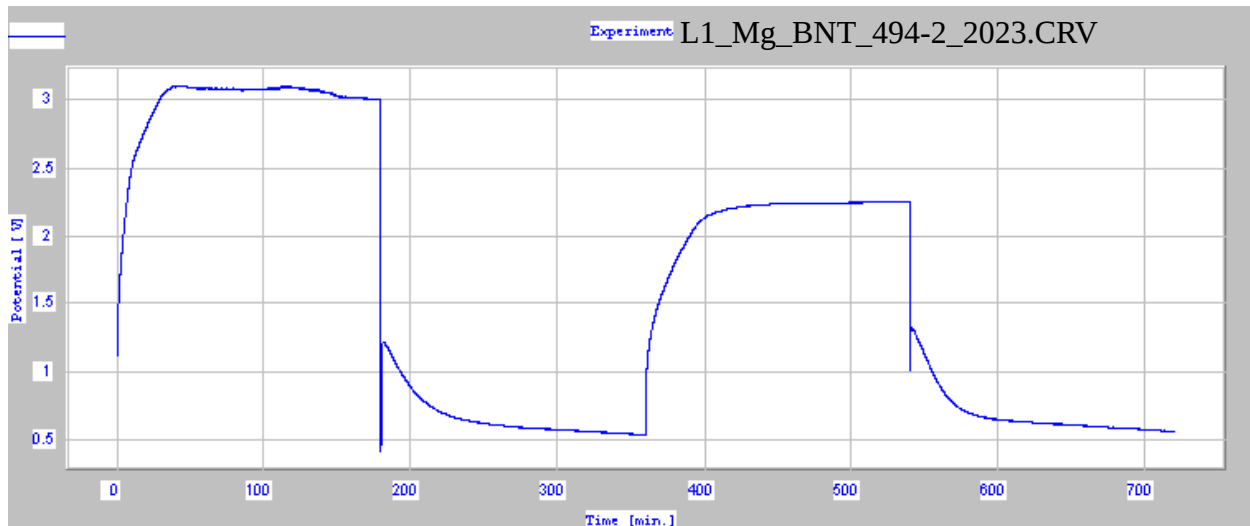


Figure 5: Cycling of Mg, BCNT cell using Electrolyte 494-2 C/D @ 100 microamps

This cell was cycled 18 times discharging at 100 microamps for three hours. As can be seen, both charging and discharging resulted in minimal polarization of the cell. The average discharge capacity of this cell was calculated to be 150 mAh/g based on the weight of the cathode material. The drawback of this system is the relatively low discharge voltage (~0.7V)

Further evidence of the importance of the supporting salt in the electrolyte is provided in the next figure. In this experiment, we compare the performance of the MgIm salt obtained from Covalent Associates (CA) with that synthesized in-house. Other than the supporting salt and the cycle times, the test conditions were identical.

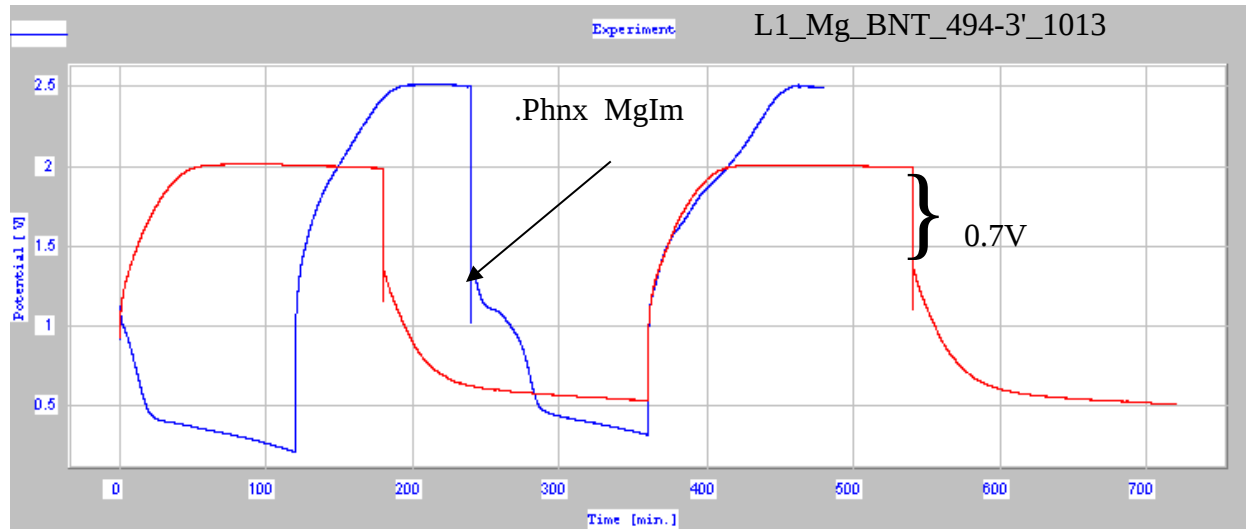


Figure 6: Comparison of the performance of two MgIm salts

As can be seen, the cell containing the CA MgIm electrolyte, was cycled for an hour longer than the cell containing the Phoenix MgIm electrolyte. Several attempts were made to prepare MgIm in-house, several products failed to perform at all. It would appear that the synthesis of this material is temperamental.

Commercially-available MgTf yielded more reliable, albeit less impressive cycling results as illustrated in the next figure. In this figure, MgTf was dissolved in the SM481-1E solvent which was a 90:10 combination of the PEG phosphate ester and the brominated phosphate ester.

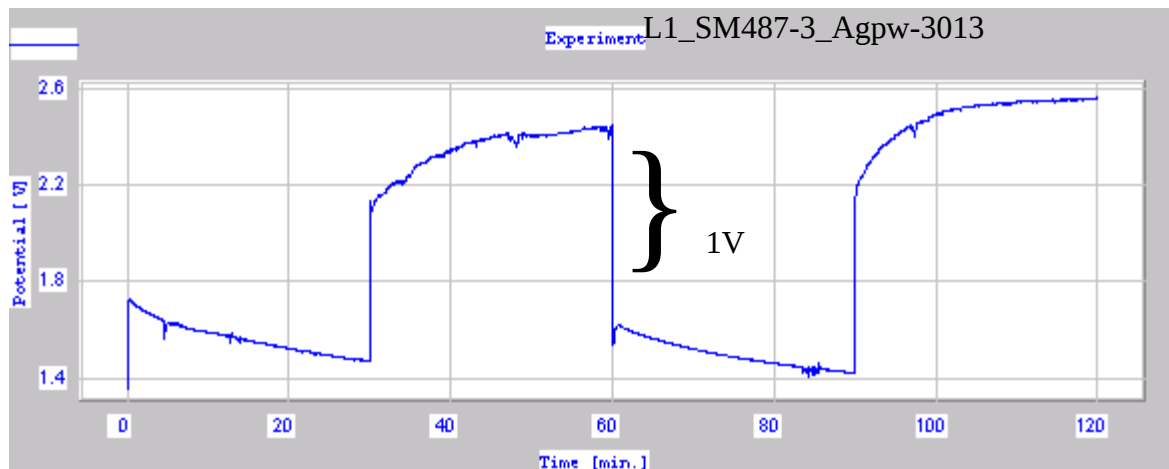


Figure 7: MgTf salt with AgO cathode D @ 100 microamps C @ 25 microamps

Here the cell rate is quite low (25 microamps and the cycle time is relatively short (30 minutes). At AgO powder cathode and a Mg anode completed the cell. Nevertheless, the under these conditions, the cell performed reasonably well attaining >1V on discharge. This can probably be attributed to the higher voltage of the AgO cathode. The IR drop of the MgTf electrolyte appeared to be far greater than that of the MgIm electrolyte as evidenced by the >1V IR drop upon discharge versus ~ 0.7V IR drop in the MgIm cell (Figure 6). The load on the MgIm cell was four times that of the MgTf cell. Following the initial voltage reversal (discharge or charge) the cell's voltage stabilized. Progressive cell polarization was undoubtedly due to the overall irreversibility of this couple; probably due to the progressive passivation of the Mg anode by reaction products. It is well known that plating of Mg is difficult process under the best of conditions. It is reasonable to assume; therefore, that the anode continues to be the center of the difficulties with the phosphate ester solvents.

Figure 8 depicts the performance of a cell containing MgIm dissolved in a commercial brominated phosphate ester (Diethyl bromopropane phosphonate) employing a B-doped CNT cathode and a Mg anode. The cell was cycled at 100 microamps, eight two-hour cycles are shown in this figure.

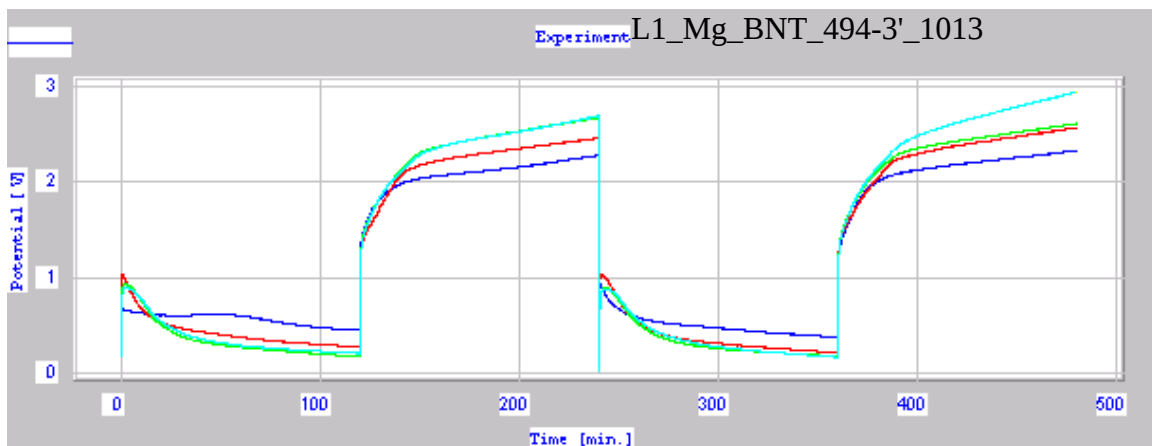


Figure 8: Cycling of a commercial solvent/ MgIm electrolyte

As can be seen, the cell discharged to a voltage of around .5V and the performance was reasonably reproducible. Over time the cell performance degenerated further; however. Here again, the electrolyte IR drop appears to be around 0.7 V and the cell polarized over time. Figure 9 below compares the anode used in this test with a fresh Mg anode.



Figure 9: Electrolyte 494-3' Anode versus a Fresh Mg Anode.

In this photograph, note the degree of corrosion product on the test anode. As can be seen here there is evidence of plated metal in the center of this electrode and evidence of corrosion products at the edges of the electrode. Based on this photograph, there can be little doubt that the electrolyte in this test was very active in transporting Mg^{+2} between the test electrodes.

Since the activity of the Mg anode appeared to be the limiting factor in obtaining a more reversible couple, attempts were made to modify the Mg to make it more active during the cycling process. To this end, we experimented with preparing Mg Li alloys as previously described. The next figure details a cycling experiment employing one of these alloys (90:10, Mg:Li) together with a vanadium phosphate/carbon black cathode and a phosphate ester/MgIm electrolyte. This cell was cycled at 50 microamps and displayed a very flat initial discharge curve. Subsequent charging yielded a small IR drop and less polarization on charge than that seen with pure magnesium. These results seemed to suggest that alloying the magnesium with lithium aided in the plating of the magnesium upon the charging of the cell.

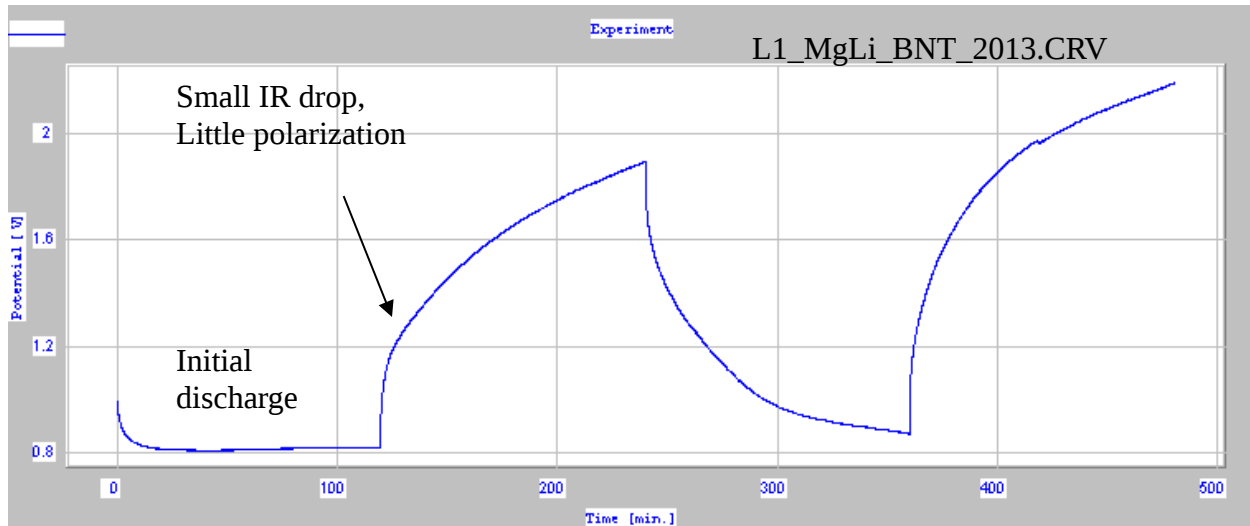


Figure 10: MgLi Alloy anode Initial Cycle

Subsequent cycling of the cell dispelled some of this notion as seen in the next figure.

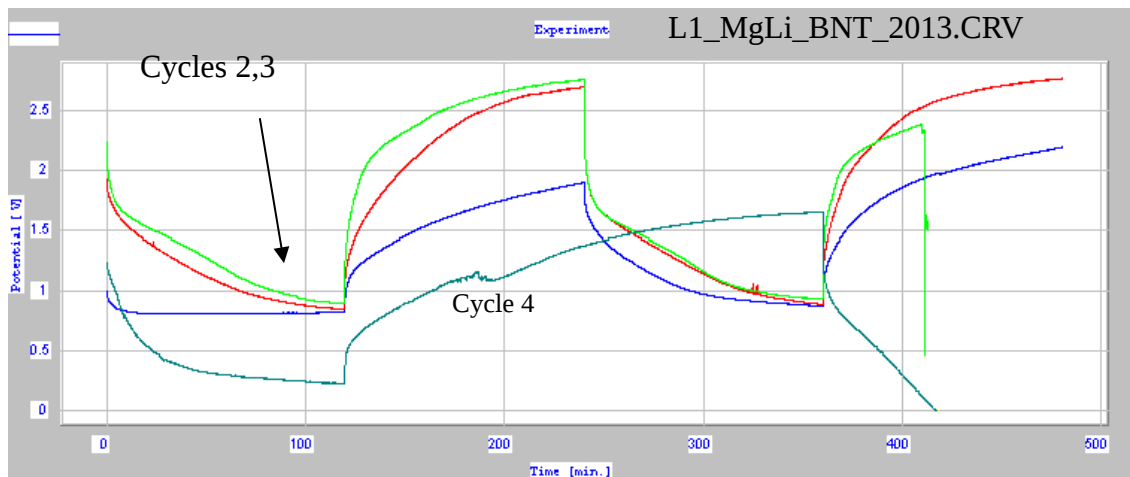


Figure 11: MgLi Alloy Anode Subsequent Cycling

As shown here, the cell performance at cycles 2 and 3 appeared to be somewhat reproducible, but by cycle 4, the cell polarized and the performance diminished appreciably.

The following figure represents some of the better results obtained during this program. In this instance, an AZ91 anode was combined with a 2mg cathode containing 80% vanadium phosphate, 20% Super P carbon black. The electrolyte was composed of MgIm in the SM481E electrolyte. The cell was cycled at 100 microamps for 3 hours.

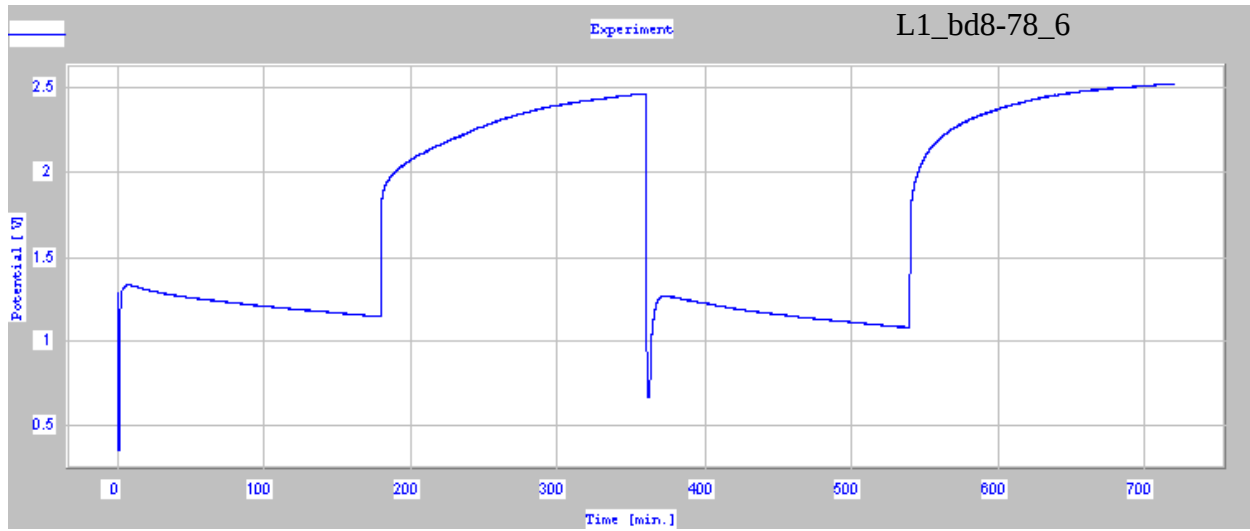


Figure 12: AZ91 Anode Initial Cycle

As shown in this figure, this cell is quite well behaved with fairly flat discharges and moderate polarization upon recharge. Subsequent cycling as seen in the next figure indicated continuation of these trends.

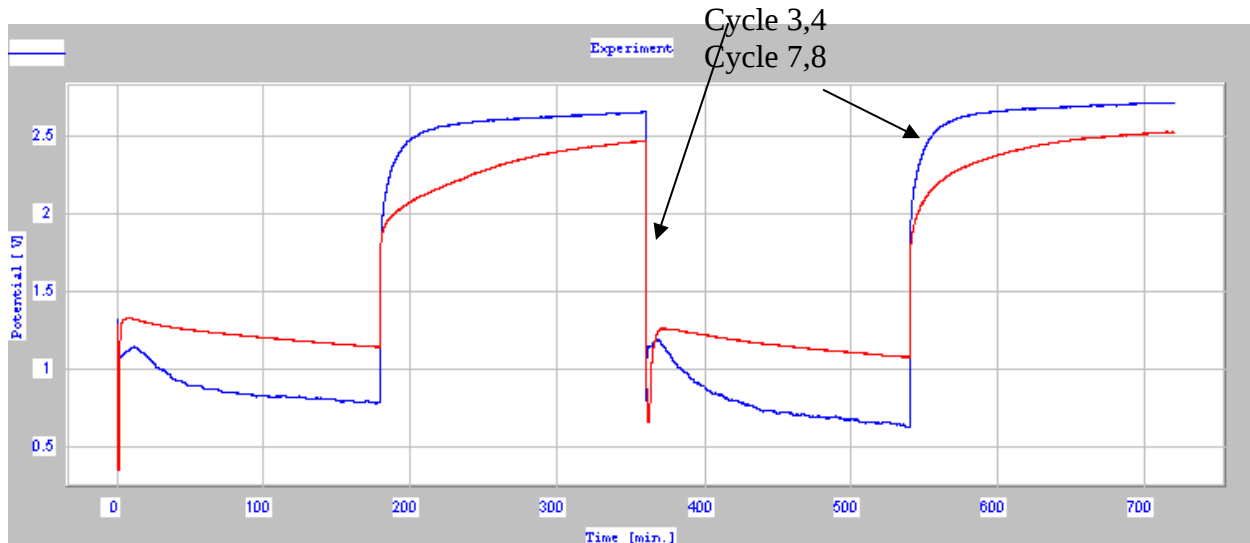


Figure 13: AZ91 Anode Subsequent Cycling

Note that with Mg alloy, the cell voltage diminishes on discharge with subsequent cycling, but upon recharge, the cell voltage flattens out at around 2.7V. Not the case with the pure Mg anode where the cell continues to polarize upon recharge (see above) this appears to indicate that the Mg alloy is more reversible as an anode than the pure Mg anode.

In the next figure, we added an ionic liquid to the electrolyte used in the previous cell and tested the system again. In this experiment, 5% butylmethyl Imid TFB was added to the MgIm phosphate ester electrolyte and the cell was charged at 150 microamps, discharged at 100 microamps. These cycles were short (30 minutes) but as shown, the cell's average discharge voltage exceeded 1 V and although the performance deteriorated somewhat with time, the cell voltage remained above 1 V on discharge.

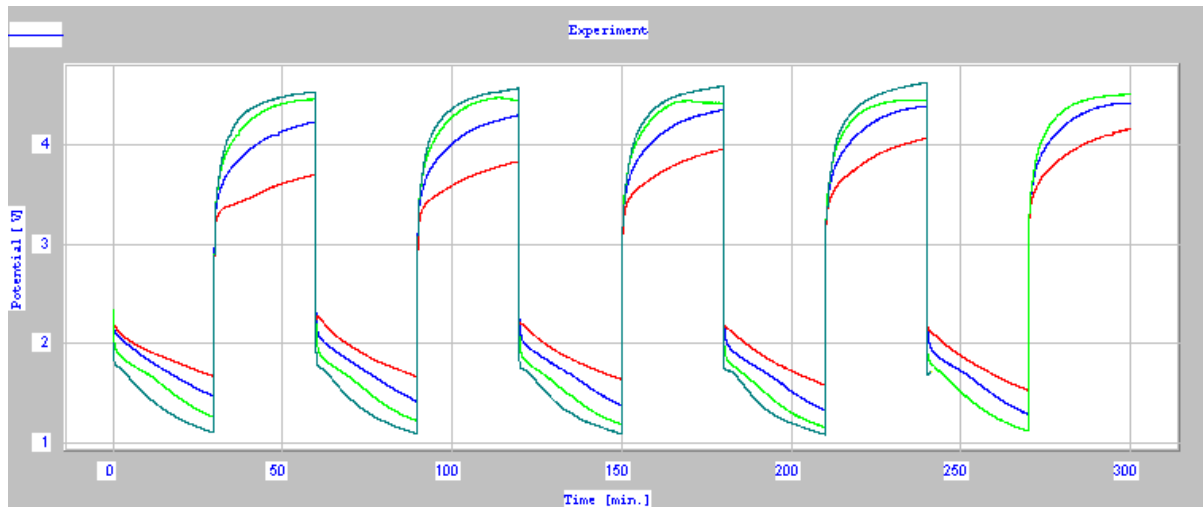


Figure 14: Ionic Liquid Electrolyte/Magnesium Cell

It would appear that inclusion of an ionic liquid in the electrolyte improved the cell performance at the expense of electrolyte conductivity as evidenced by the increased IR drop exhibited by this cell.

3.0 MAGNESIUM BATTERY EFFORT CONCLUSIONS AND RECOMMENDATIONS

- 1) Magnesium imide dissolved in a phosphate ester solvent that contains a halogenated phosphate ester appears to be the preferred electrolyte for a rechargeable Mg cell.
- 2) A combination of B-doped CNTs and vanadium phosphate appear to be the cathode of choice for a rechargeable Mg cell by virtue of higher voltage and better reversibility.
- 3) Magnesium alloys appear to perform better in a rechargeable system than pure magnesium, possibly due to absence of passivation upon plating of the magnesium on the alloy.

Recommendations:

- 1) Investigate synthesis of MgIm and how to improve its purity.
- 2) Investigate combinations of halogenated phosphate esters and MgIm as improved electrolyte.
- 3) Further investigate vanadium phosphate as a cathode material.

4.0 SUPERCAPACITOR RESEARCH EFFORT

Summary of Results & Recommendations

We have established that our phosphonate-based electrolytes possess voltage stabilities of substantially ***greater than 10V***. This voltage stability is far superior to state of the art electrolytes that are limited to a maximum useful voltages of ~3.5-4V. In addition, the capacitances attained with the phosphonates were sometimes found to be qualitatively higher than those of state of electrolyte systems which were run as controls.

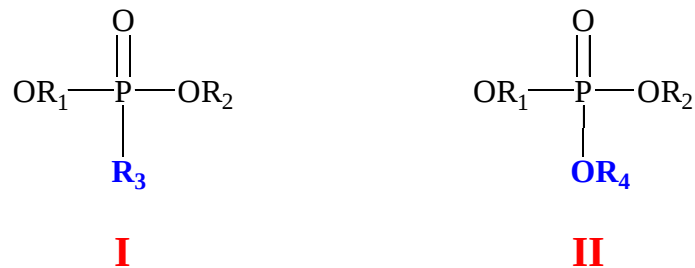
Our explorations suggest that with our high voltage electrolyte the supercapacitor performance is limited by the electrode materials and overall capacitor design. We recommend that an expanded R&D program be undertaken by Phoenix Innovation in which the electrodes are optimized to match our phosphonate/phosphate electrolyte performance. Although outside the scope of the funded effort, early experiments in our laboratories have turned up a number of promising electrode electrode design leads.

4.1 Results & Discussion

The work was split into three basic areas, phosphonate chemistry and electrochemical design, followed by the critical performance evaluations. State of the art supercapacitor electrolytes were used as absolute controls in these experiments. The following sections summarize the best of our results to date.

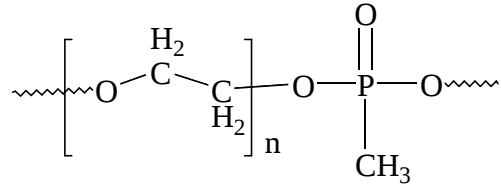
Chemistry

Two basic types of phosphorous esters were explored, phosphonates (**I**) and phosphates (**II**):



R_1, R_2, R_3 & R_4 are alkyl, aryl or mixed alkyl-aryl

In addition to these simpler compounds, oligomeric and polymeric phosphorus ester compounds have been prepared as well. By way of example:



All of these compositions have promise as supercapacitor electrolytes. Naturally, the brief nature of this effort only allowed for the study of a relatively few compositions. Almost certainly an expanded effort will discover improved solvent materials and electrolyte formulations derived therefrom.

4.1.1 Conductivity

The electrolytes' conductivity varied as shown in Table 1, and matched up well with state of the art electrolytes. Especially noteworthy is that the experimental phosphorus ester-based electrolytes, *Phnx 2* and *Phnx 2802*, yielded conductivities within a factor of two of that of the

corresponding ammonium salt system. Since the former are surely not optimized, this result bodes well for future improvements in conductivities for these novel electrolytes.

*Table 2: Representative Electrolyte Conductivities (22°C)**

Supporting Salt	Solvent	Resistance (Ω)	Conductivity (S/cm)
1M LiPF ₆	MeCN	5.5	5.5x10 ⁻³
1M SbF ₆	Phnx 2802	27.8	1.1x10 ⁻³
1M TBATFB	MeCN	10.4	2.9x10 ⁻³
1M LiPF ₆	Phnx 2	10.2	2.9x10 ⁻³

* TBATFB = tetrabutylammonium tetrafluoroborate; MeCN = acetonitrile

4.1.2 Cyclic Voltammetry:

The purpose of the CV tests was to determine if the electrode pairs developed capacitance at high voltage and to compare the relative performance of control electrolytes with that of the experimental electrolytes. Figure 15 is a typical CV for an experimental capacitor electrolyte consisting of 1M lithium salt dissolved in the Phoenix solvent together with graphite/carbon black powder electrodes.

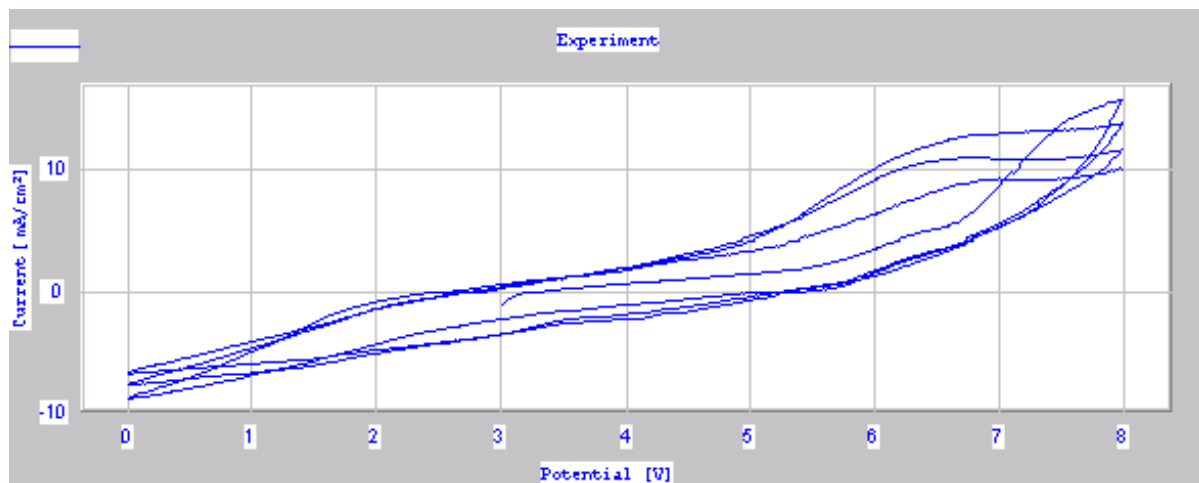


Figure 15: CV of Experimental Electrolyte

This figure demonstrates that the experimental electrolyte can easily withstand voltage sweeps of up to 9V with little decomposition as would be evidenced by high current generation. In

addition, the current (i) hysteresis of the CV curve over the entire voltage range is an indication of the relative capacitance of the system. This same test was conducted with a control electrolyte consisting of the 1M lithium salt dissolved in acetonitrile and the same test electrodes. These results are combined with those of Figure 1 for comparison in Figure 2:

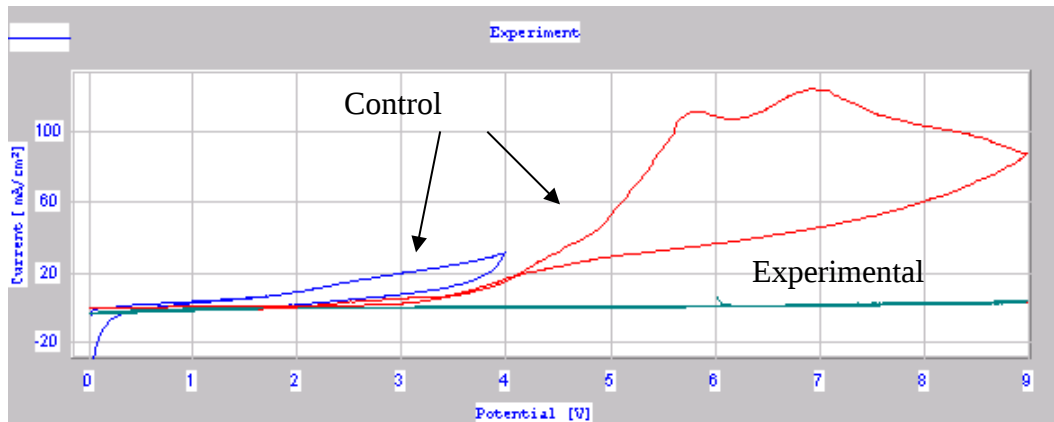


Figure 16: Comparison of CVs for Test and Control Electrolytes

There are several interesting points about Figure 2. First, it is clear that the control electrolyte behaves very well over the narrow voltage range from 0 to 4 V as evidenced by a wide and well-behaved current (i) hysteresis over this range. Beyond 5 V however, the CV shows very high ($>100\text{mA}$) currents are generated, indicative of solvent decomposition. Contrasted with this behavior is that of the experimental electrolyte at the bottom of the figure. This curve is a replot of Figure 1 and as can be seen, there is 10 times less current developed in the 5 V to 9 V region of the CV, indicative of phosphate solvent stability. The downside of the result is that the current hysteresis of the experimental electrolyte is not as great as that of the control electrolyte. This would mean that although there is capacitance in the system at these higher voltages, it doesn't appear to be of the same magnitude as that of the control. This may be due to lower ionic conductivity in the experimental electrolyte.

4.1.3 Chronopotentiometry:

Following the CV experiments, cycling experiments were conducted with a number of electrolyte candidates. Figure 3 is a typical cycle curve for a control electrolyte.

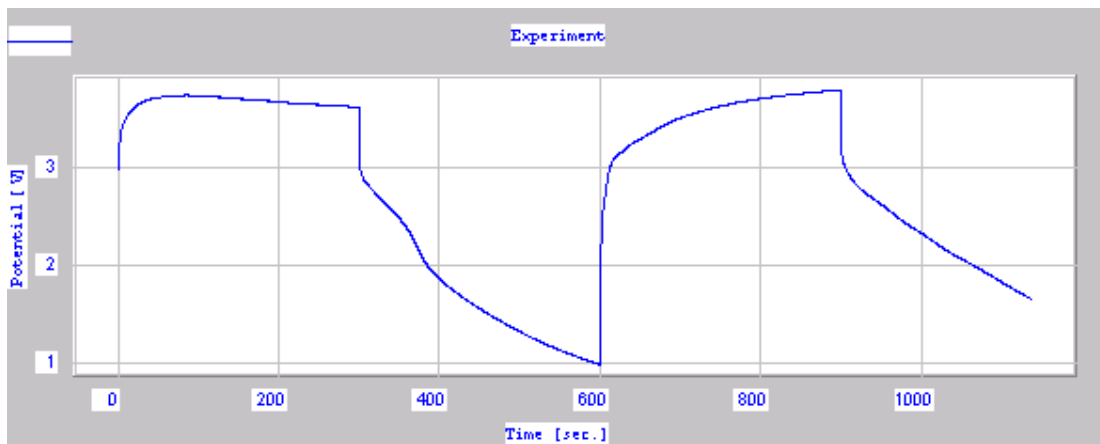


Figure 17: 1M Lithium Salt in Acetonitrile, Control

This particular control test shows that the cell will not achieve voltages much higher than 4 V even when the cell is subjected to 15 mA of charging current. Upon discharge at 0.5 mA, a significant IR drop is observed, indicative of crude electrode structure, and the cell then discharges exhibiting significant capacitance.

A direct comparison of the control electrolyte results of Figure 3 with several experimental electrolytes is given in Figure 18

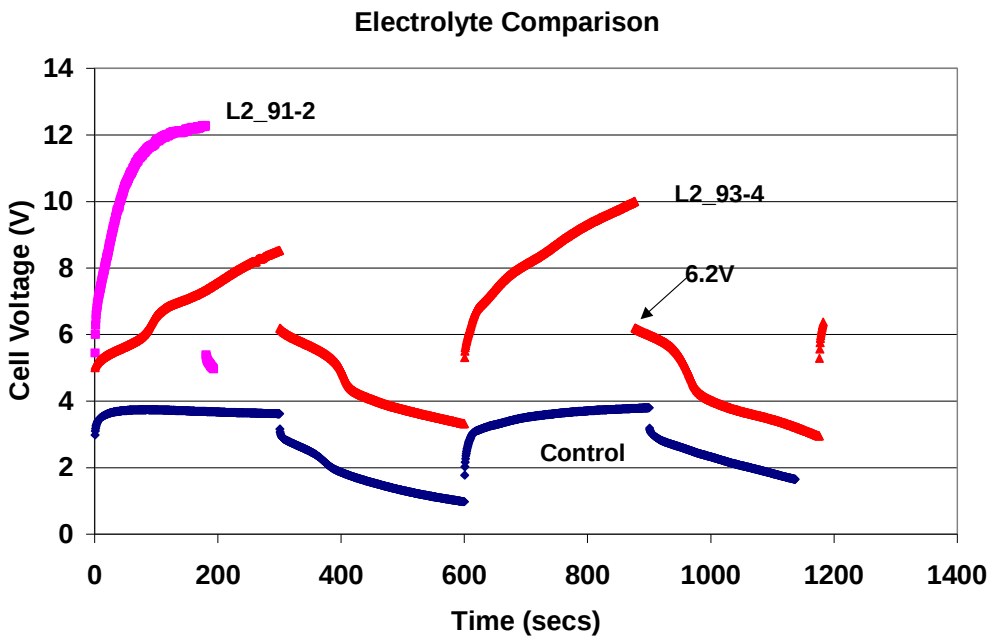


Figure 18: *Chronopotentiometric Tests of Various Electrolytes*

In Figure 18, the charge and discharge currents for these test cells were the same and the electrodes used were the same. The control test is a replot of Figure 17, but as can be seen, the experimental phosphonate electrolytes (L2-912-2 and L2_93-4) attain far greater voltage than the control electrolyte under the same test conditions. The experimental cell labeled L2_93-4 attained **10 V** by the second cycle and the cell L2_91-2 attained **12V** on the first cycle. Upon discharge, the 10 V cell attains 6.2 V and exhibits far greater capacitance than the control cell. The IR drop for both of the experimental cells is very significant (>3.5V), but may be ameliorated with better electrode design, as well as higher electrolyte conductivity, the latter possibly achieved through better supporting salt design.

Figure 19 is presented to illustrate that the experimental electrolyte can maintain stability at nearly 10 V for a substantial period:

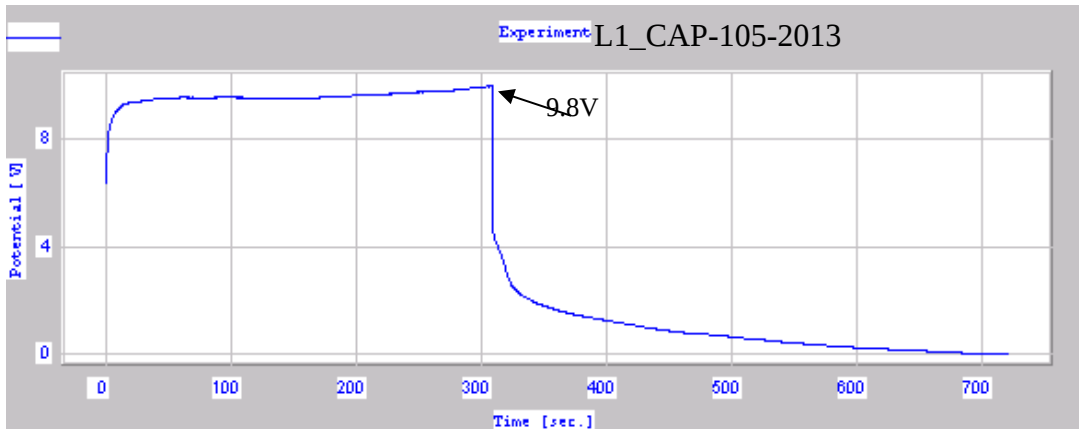


Figure 19: *Experimental Electrolyte charged to 9.8 V*

With respect to improved IR drop, Figure 20 is for an experimental electrolyte of slightly modified composition.

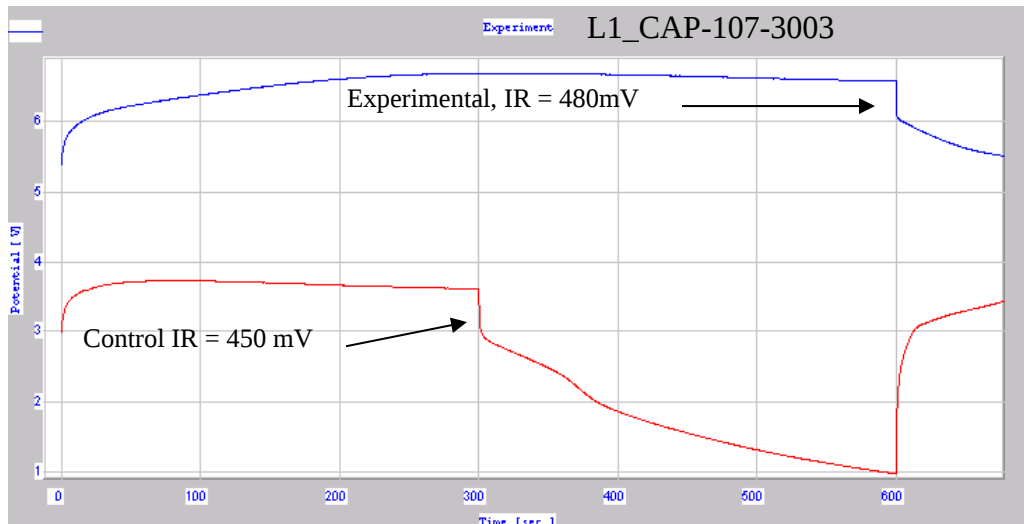


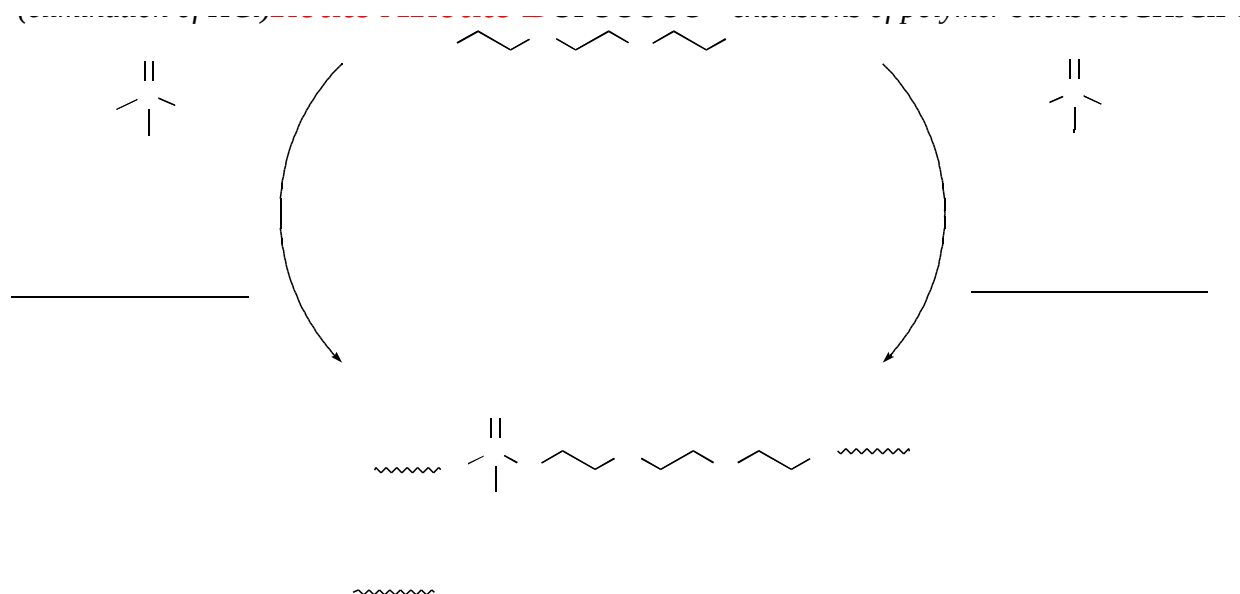
Figure 20: *Modified Experimental Electrolyte*

This Figure is an indication that the electrolyte could be further improved as evidenced by an IR drop of only 480 mV following the charging of the cell to >6.5V. This is quite a favorable result, especially when compared to the control which was charged to 3.5 V and exhibited an IR drop of 450 mV.

4.2 Experimental

4.2.1 Syntheses & Purifications

Established synthetic techniques were used to prepare the phosphonate and phosphate solvents tested by one of two procedures, generically shown hereafter for the case of a typical polyphosphonate product:



Route A involves the virtually instantaneous reaction of an acid chloride with a diol, in the presence of an acid scavenging base. Route B is a transesterification involving the elimination of the small product molecule methanol, whose removal drives the reaction.

Where necessary, the compounds were purified by column chromatography and/or vacuum distillation. The lithium and ammonium salts were purchased from Aldrich or Alfa Chemicals, and used as received.

4.2.2 Electrochemistry:

All of the experiments were conducted under ambient conditions on the lab bench using a Radiometer Voltlab PGZ 301 electrochemical test apparatus. Chronopotentiometry was conducted on the electrode pair by impressing specific charge and discharge currents while monitoring the cell voltage. Plots of cell voltage versus time were recorded. Over one hundred different combinations of electrolytes and electrodes were tested in a 30 day period during this effort. A simple two-electrode test cell utilizing stainless steel piston current collectors in a

polypropylene sleeve with a steel pressure clamp cell holder was used to test the electrolytes. Graphite powder, carbon black (Super P, SA \sim 60m²/g), and single wall carbon nanotubes were examined as active electrode materials. In all of the experiments, the active electrode powder was supported on an inert material, such as pure gold or platinum metal backing, to prevent corrosion of the stainless steel current collectors. Cells were charged using various currents ranging from 1 to 15 mA. Discharge currents ranged from 0.5 to 1.0 mA. Multiple charge/discharge cycles were imposed on the better candidate electrolyte to ascertain their relative stability.

Cyclic voltammetry was performed using the same test cell configuration as the chronopotentiometry tests. Cyclic voltammetry was performed at a sweep rate of 50 mV/sec over various voltage ranges under ambient conditions.

Conductivity measurements were made using the two 1cm² stainless steel electrode cell with one piece of separator. This cell was pressed using constant pressure from a mechanical cell holder. The separator was wetted with the test electrolyte and the impedance of the electrolyte was determined using a Phillips model 6303A PCL meter. The conductivity of the electrolyte was then calculated from the thickness of the separator and the measured cell resistance.

5.0 CONCLUSION

This brief research effort has established that Phoenix Innovation's family of phosphonate/phosphate electrolytes can be used in supercapacitor systems at voltages of greater than 10V. This was the objective of the work.

¹ Aurbach, D.; et al., *J. Power Sources* **97-98** 28 **2001**.

² Novak, P.; et al., *Elec. Acta* **45** 351 **1999**.

³ Yoshimoto, N.; et al., *Elec. Acta* **48** 2317 **2003**

⁴ Oh, J-S.; et al., *Elec. Acta* **50** 898 **2004**.

⁵ Chusid, O., et al.; *Adv. Mater.* **15** 627 **2003**.

⁶ Aurbach, D.; et al., *Nature* **407** **2000**.

⁷ <http://www.dot.gov/affairs/faa001.htm>